Catalysis Letters Vol. 87, Nos. 1–2, April 2003 (© 2003)

AFM and XPS study of the sintering of realistic Ag/{0001}α-Al_2O_3 model catalysts under conditions of ethene epoxidation

Stefan Wodiunig, James M. Keel, Tamsyn S.E. Wilson, Fessehaye W. Zemichael, and Richard M. Lambert *

Chemistry Department, Cambridge University, Cambridge CB2 1EW, UK

Received 8 November 2002; accepted 21 January 2003

The stability under reaction conditions of realistic Ag/α-alumina model catalysts prepared by an appropriate wet chemical route has been studied by AFM and XPS. Although thermal and oxygen-induced sintering of Ag particles on {0001}α-alumina are significant, parts per million levels of dichloroethane have a much larger effect. It is suggested that this latter effect is due to AgCl-mediated intra-particle transport of silver. Such chlorine-induced sintering is likely to be the principal cause of the loss of Ag metal area under industrial conditions.

KEY WORDS: AFM; XPS; silver; α-alumina; 1,2-dichloroethane; epoxidation; ethane; sintering.

1. Introduction

In addition to activity and selectivity, the useful lifetime of industrial heterogeneous catalysts is a critically important factor in the overall process economics. In the case of Ag/α-alumina catalysts used for the catalytic epoxidation of ethene, a useful lifetime of the order of two years is required for commercial viability. However, relatively little is known at the fundamental level about the relative importance of the various factors that determine catalyst decay in this case, or indeed in many other cases. In the case of Ag/α-alumina, these factors include metal particle sintering, adsorption of poisons and the loss or redistribution of promoter species: with silver, there is no doubt that a major cause of activity decay is sintering of the metal particles [1–3]. Thus, for example, previously [3] we examined the sintering of silver using dispersed Ag/α-alumina catalysts extensively aged under actual industrial conditions.

We have shown [4] that realistic Ag/α-alumina model catalysts may be prepared on single-crystal faces of α-alumina by following the same wet chemical and calcination procedures that are used in the preparation of the corresponding practical dispersed catalysts. The properties of such realistic model catalysts may differ very substantially from those of the notionally equivalent systems prepared by vacuum deposition of Ag on α-alumina [5]. Here we extend this approach to investigate some of the factors that can affect the stability and sintering of Ag particles on well-defined {0001}α-Al_2O_3 surfaces under conditions relevant to the epoxidation of ethylene. AFM and post-reaction XPS were used to investigate sintering effects resulting from exposure to reaction gas. Not unexpectedly, temperature plays a role, as does the presence of oxygen. However, the most import effect is caused by parts per million levels of dichloroethane (DCE), used industrially to deposit the chlorine promoter which is vital to commercial operation.

2. Experimental

{0001}-oriented single-crystal α-alumina samples supplied by PI-KEM with dimensions of $10 \times 10 \times 0.5$ mm were used. Prior to Ag precursor deposition, samples were cleaned with 50% nitric acid, distilled water and acetone and dried for 12 h at 360 K, following the procedure of Bird *et al.* [4]. They were then annealed in air at 1700 K for 15 h to create a smooth, defect-free surface. Images were taken under ambient conditions using a ZEISS-BEETLE instrument in the non-contact AFM mode. The AFM quartz needle sensors fitted with silicon tips for improved resolution were fabricated and supplied by Johnson's group at the University of Pennsylvania [6].

$AgNO_3$ (Aldrich) was used as the silver precursor [7–9]. By means of a micro-pipette, a 1 μl droplet of a 5.8×10^{-10} mol aqueous solution was deposited on each of three alumina samples held at ~350 K. This procedure was calculated to generate silver loadings of a similar order of magnitude to those used in the industrial catalyst (~16 wt% or 40.5 $\mu g\,cm^{-2}$).

2.1. Treatment of the Ag/{0001}α-Al_2O_3 samples

Following industrial practice, all three samples (denoted S1, S2, S3) were calcined in nitrogen by heating at 773 K for 12 h so as to decompose the nitrate to metallic Ag [10]. The calcined samples were then subjected to a

---

* To whom correspondence should be addressed.
E-mail: rml1@cam.ac.uk

1011-372X/03/0400-0001/0

series of procedures that were carried out in a well-mixed quartz reactor operated at atmospheric pressure. Start-up and aging procedures were chosen so as to mimic the conditions encountered in ethylene epoxidation catalysis. Samples S2 and S3 were then heated ($5\,\mathrm{K\,min^{-1}}$) and aged in reaction mixture with and without DCE, respectively, at 513 K for 25 h. The reaction gas was delivered by means of electronic mass-flow controllers (Brooks 5850 TR) at a total flow rate of 100 STP $\mathrm{ml\,min^{-1}}$ and consisted of 8% O_2, 20% C_2H_4 (BOC Gases UK) and balance He. When used, DCE (Messer UK) was supplied at a concentration of 1.2 ppm, in line with the industrial procedure for supplying chlorine promoter to the catalyst [11]. Sample S1 was used as a control: it was subjected to the same treatment as S2 and S3, but using nitrogen rather than reaction gas. AFM images were obtained after each step of the above procedures.

2.2. X-ray photoelectron spectroscopy

Post-reaction XPS measurements were carried out using a VSW ARIES system equipped with an HA-100 hemispherical analyzer. The alumina single-crystal samples were held in an aluminum sample holder, their dimensions being larger than the X-ray spot size. The XP spectra were recorded using MgKα radiation and quoted binding energies are referred to the C 1s emission at 284 eV.

3. Results

Figure 1(a) shows an AFM image of the clean and freshly annealed {0001}Al_2O_3 surface. The clean surface exhibits a characteristic step and terrace features

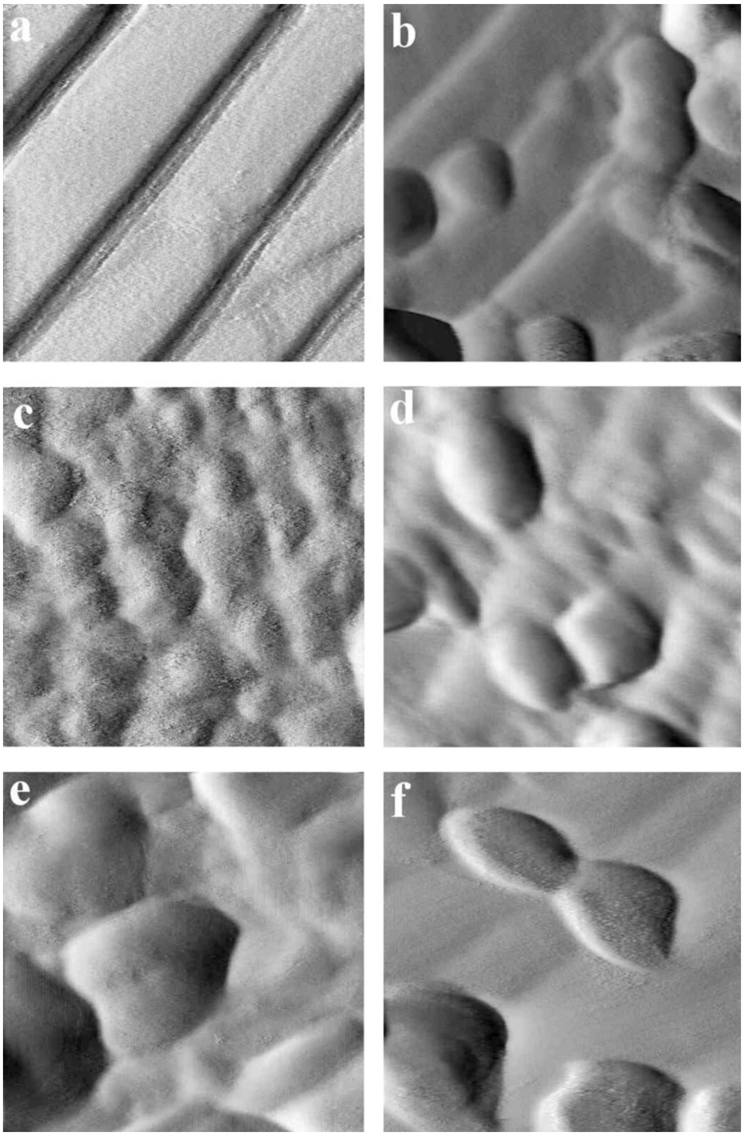

Figure 1. AFM images (630 nm × 630 nm) of Ag/α-Al_2O_3 (0001) single-crystal samples aged at 513 K for 25 h under different conditions: (a) clean; (b) deposited with silver and calcined in nitrogen at 773 K for 12 h; (c) S1 calcined in nitrogen at 513 K for 25 h; (d) S2 treated in a reaction mixture at 513 K for 25 h; (e) S3 treated in a reaction mixture including 1.2 ppm of DCE at 513 K for 25 h; (f) heated in 8% O_2 at 553 K for 25 h.

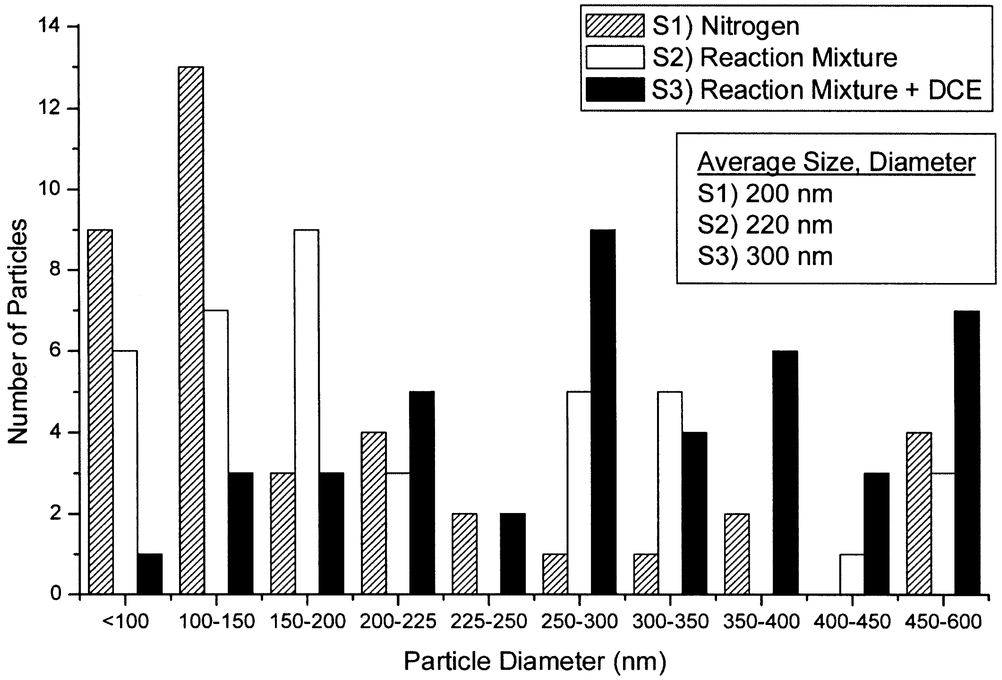

Figure 2. Histogram illustrating silver particle size distribution. S1, calcined in nitrogen at 513 K for 25 h; S2, treated in a reaction mixture at 513 K for 25 h; S3, treated in a reaction mixture including 1.2 ppm of DCE at 513 K for 25 h.

structure that is in good agreement with the results of Beitel *et al.* [5] and Bird *et al.* [4]. The 50–100 nm wide {0001} terraces are separated by step edges 2–3 nm high, which comprise $(11\bar{2}0)$ and $(\bar{2}110)$ planes. Figure 1(b) shows an AFM image obtained after calcination of the Ag nitrate deposit in N_2 at 773 K for 12 h. The silver particles were of height 5–10 nm and all three samples had very similar morphologies after this initial calcination step. Some crystallites exhibited faceted edges whose symmetry suggests that the {111} plane of Ag was in contact with the {0001} alumina surface. Subsequently the three samples were treated at 513 K for 25 h with gas mixtures of three different compositions. As a control, sample S1 was treated in flowing pure nitrogen. As described in section 2, sample S2 was treated with 100 STP ml min^{-1} of reaction mixture, and sample S3 was similarly treated with reaction mixture to which 1.2 ppm DCE had been added. It is apparent from figure 1(c) that thermal treatment in an inert atmosphere resulted in negligible Ag particle growth over the experimental time scale. Treatment with reaction mixture did result in measurable metal particle growth (figure 1(d)), which we ascribe to the effect of oxygen-induced sintering. This is confirmed by the image shown in figure 1(f), which resulted from subsequent treatment of control sample S1 with 8% oxygen at 553 K for 25 h. The most striking result is that shown in figure 1(e), which reveals that even modest exposure to reaction mixture containing 1.2 ppm DCE results in very substantial Ag particle growth. Clearly, the sintering behavior of the system is very sensitive to the presence of tiny amounts of the promoting chlorocarbon.

The silver particle size distributions obtained from the AFM images for the three samples S1, S2 and S3 are illustrated in figure 2, and the average Ag particle diameters are listed in table 1. The latter were derived by counting particles from 10 different areas for each sample. It is apparent that although exposure to reaction gas significantly increased the average Ag particle diameter, addition of DCE to the reaction gas markedly accelerated the sintering of silver.

The corresponding XP spectra were dominated by the Al(2p) and O(1s) emission at 77 and 531 eV, respectively, along with a peak at 367 eV, the Ag(3d) emission characteristic of metallic silver. This observation, together with the absence of N(1s) emission in the region of 400 eV, confirms complete conversion of the nitrate to the metal during the initial calcination step.

Table 1
Average Ag particle diameters derived from the data shown in figure 2

Sample/treatment	Mean particle diameter from AFM data (nm)	Mean particle diameter deduced from XPS intensities (nm)
S1/nitrogen	200	200[a]
S2/reaction mixture	220	220
S3/reaction mixture + DCE	300	350

[a] Set equal to the AFM-derived value.

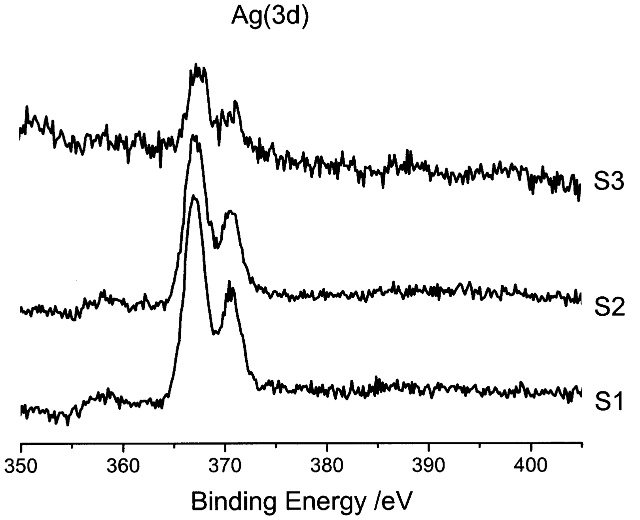

Figure 3. X-ray photoelectron Ag(3d) spectra for a series of Ag/Al_2O_3 (0001) single-crystal samples. S1, calcined in nitrogen at 513 K for 25 h; S2, treated in a reaction mixture at 513 K for 25 h; S3, treated in a reaction mixture including 1.2 ppm of DCE at 513 K for 25 h.

The XP spectra obtained from the variously treated samples are shown in figure 3 and are consistent with the AFM results. The XPS results give a macroscopic area-integrated picture of the sample condition and therefore provide a valuable check on the degree to which the AFM images are representative of the whole sample. Recall that the technique is fairly surface sensitive, so that sintering of the silver particles should manifest itself as a decrease in the integrated Ag(3d) emission intensity. This is indeed observed. Thus the intensity from S2 (reactions gas) is measurably lower than that from S1 (N_2 control). Strikingly, the intensity from S3 (reaction gas + DCE) is lowest of all by a substantial margin, clearly confirming the AFM result that traces of chlorocarbon are the single most important factor leading to Ag particle growth. The XPS intensities may be used to estimate the variation of mean Ag particle size according to a simple model based on two assumptions. Firstly, that the silver is present as mono-dispersed hemispherical particles. Secondly, that the Ag(3d) emission from each particle originates from a maximum depth of 7 nm (the effective sampling depth of Ag(3d) photoelectrons). Normalized estimated diameters for samples S2 and S3 were then calculated by associating a diameter of 200 nm (based on the AFM result) with the measured Ag XPS intensity from sample S1, and the results are given in table 1. A relatively small increase in estimated particle diameter is observed between the control sample S1 and sample S2 (run in reaction mixture) from ~200 nm to ~220 nm. However, in agreement with the AFM result, the presence of DCE in the reaction mixture resulted in very pronounced Ag particle growth to an estimated diameter of 350 nm.

4. Discussion

The oxygen-induced sintering of Ag is well known [4,12,13] and it is therefore not surprising to see that our model catalysts also exhibit this behavior. Our most significant finding concerns the pronounced adverse effect of DCE on the rate of Ag sintering. DCE deposits chlorine adatoms on the Ag surface [14–17], increasing the electrophilicity of O_a and thus enhancing epoxidation of ethene at the expense of combustion [18]. With ethene and oxygen alone, selectivities in the order of only ~50% are achievable; addition of DCE raises the selectivity to >75% which represents a huge commercial advantage. This is why DCE or similar chlorocarbons are essential additives in the industrial operation of Ag/α-alumina ethene epoxidation catalysts. However, the present results make it clear that this large gain in selectivity is obtained at the cost of accelerated activity loss through Ag sintering. Under industrial conditions, this activity loss may be counteracted to some extent by increasing the reaction temperature; however, this decreases selectivity and accelerates sintering.

Little or nothing appears to be known about the mechanism of Ag sintering on α-alumina under any conditions. Here, we are principally concerned to understand the very large effect of DCE on Ag particle growth. Recent Auger spectroscopy and STM results for Ag(111)/Cl show that after sufficiently large exposures ($\sim 10^5$ Langmuirs) to chlorine gas at room temperature, nucleation and growth of AgCl islands occurs on the metal surface [19–22]. In the present case, assuming that each impinging DCE molecule deposits one chlorine atom with unit probability, the effective total chlorine dose received by the model catalysts is of the order of $\sim 10^8$ Langmuirs. Thus even if the reaction probability of each impinging DCE molecule at 513 K (as opposed to room temperature) is only of the order of 10^{-3}, nucleation and growth of AgCl islands seems likely under the conditions of our experiments. (In this connection, note that under industrial conditions the partial pressure of DCE is ~20 times higher than in our experiments.)

Therefore AgCl-mediated transport of silver is a plausible mechanism for the chlorine-induced sintering of Ag by means of a dynamic $Ag + Cl \leftrightharpoons AgCl$ equilibrium. Bonding of Ag to chlorine should weaken Ag–Ag bonding, and the interaction of AgCl with the (ionic) support should be more favorable than that of Ag metal with alumina. AgCl thus becomes the vehicle for inter-particle silver transport, probably, though not necessarily, by an Ostwald ripening process: one might expect smaller Ag particles to be more prone to chloride formation than large ones.

Finally, we emphasize that the behavior reported here is likely to be of direct relevance to an understanding of the corresponding properties of practical Ag/α-alumina dispersed catalysts because the same preparative wet chemistry applies in the two cases. Thus the state of hydroxylation of the alumina surface, and the nucleation, growth and decomposition of the metal precursor compound should also be very similar in the two cases. The same cannot be said of model systems made by direct vacuum deposition of the metal on the oxide surface: this is why we designate our samples as *realistic* model catalysts.

5. Conclusions

1. XPS and AFM data provide a consistent picture of the resistance to sintering of Ag/α-alumina catalysts prepared by a wet chemical route.
2. Although thermal and oxygen-induced sintering of Ag particles on α-alumina are significant at the temperature relevant to ethene epoxidation, these processes are not the most important ones.
3. Very small partial pressures of dichloroethane result in rapid sintering of Ag, possibly by a mechanism involving the reversible formation and subsequent transport of AgCl across the support surface. Chlorine-induced sintering is likely to be the principal cause of loss of Ag metal area under industrial conditions.

Acknowledgment

This work was supported in part by Grant No. G5RD-CT-1999-00154 awarded by the European Commission.

References

[1] D.M. Minahan, G.B. Hoflund, W.S. Epling and D.W. Schoenfeld, J. Catal. 168 (1997) 393.

[2] M.M. Bhasin, P.C. Ellgen and C.D. Hendrix, US Patent 4,916,243.

[3] N. Macleod, J.M. Keel and R.M. Lambert, Catal. Lett. (in press).

[4] D.P.C. Bird, C.M.C. de Castilho and R.M. Lambert, Surf. Sci. 449 (2000) $L_2$21.

[5] G. Beitel, K. Markert, J. Wiechers, J. Hrbek and R.J. Behm, in: *Adsorption on Ordered Surfaces of Ionic Solids and Thin Films*, Series in Surface Sciences Vol. 33, eds. H.J. Freund and E. Umbach (Springer, Berlin, 1993) p. 71.

[6] W. Clauss, J. Zhang, D.J. Bergeron and A.T. Johnson, J. Vac. Sci. Technol. B 17 (1999) 1309.

[7] R.G. Bowman, US Patent 4,845,253 (1989).

[8] P. Hayden, UK Patent 1,600,747 (1981).

[9] S.N. Goncharova, E.A. Paukshtis and B.S. Bal'zhinimaev, Appl. Catal. A 126 (1995) 67.

[10] J.W. Couves, personal communication.

[11] J.G. Serafin, A.C. Liu and S.R. Seyedmonir, J. Mol. Catal. A 131 (1998) 157.

[12] A.K. Santra, B.K. Min and D.W. Goodman Surf. Sci. 515 (2002) L475.

[13] X.F. Lai and D.W. Goodman J. Mol. Catal. A 162 (2000) 33.

[14] G. Rovida and F. Pratesi, Surf. Sci. 51 (1975) 270.

[15] G. Rovida, F. Pratesi, M. Maglietta and E. Ferroni, Japan J. Appl. Phys., Suppl. 2, Part 2 (1974) 117.

[16] G. Rovida, F. Pratesi and E. Ferroni, J. Catal. 41 (1976) 140.

[17] E. Zanazzi, F. Jona, D.W. Jepsen and P.M. Marcus, Phys. Rev. B 14 (1976) 432.

[18] R.B. Grant and R.M. Lambert, J. Catal. 92 (1985) 364.

[19] B.V. Andryushechkin, K.N. Eltsov, V.M. Shevlyuga and V.Yu. Yurov, Surf. Sci. 431 (1999) 96.

[20] B.V. Andryushechkin, K.N. Eltsov and V.M. Shevlyuga, Surf. Sci. 435 (1999) 109.

[21] B.V. Andryushechkin, K.N. Eltsov, V.M. Shevlyuga and V.Y. Yurov, Surf. Sci. 407 (1998) L633.

[22] K. Wu, D. Wang, J. Deng, X. Wei, Y. Cao, M. Zei, R. Zhai and X. Guo, Surf. Sci. 264 (1992) 249.